Published in final edited form as:
Hum Mov Sci. 2014 August ; 0: 134–153. doi:10.1016/j.humov.2014.05.007.

Online kinematic regulation by visual feedback for grasp versus transport during reach-to-pinch

Raviraj Nataraj, **Cristian Pasluosta**, and **Zong-Ming Li**
Hand Research Laboratory, Departments of Biomedical Engineering, Orthopaedic Surgery, Physical Medicine and Rehabilitation, Cleveland Clinic, Cleveland, Ohio

Abstract

Purpose—This study investigated novel kinematic performance parameters to understand regulation by visual feedback (VF) of the reaching hand on the grasp and transport components during the reach-to-pinch maneuver. Conventional metrics often signify discrete movement features to postulate sensory-based control effects (e.g., time for maximum velocity to signify feedback delay). The presented metrics of this study were devised to characterize relative vision-based control of the sub-movements across the *entire* maneuver.

Methods—Movement performance was assessed according to reduced variability and increased efficiency of kinematic trajectories. Variability was calculated as the standard deviation about the observed mean trajectory for a given subject and VF condition across kinematic derivatives for sub-movements of inter-pad grasp (distance between thumb and index finger-pads; relative orientation of finger-pads) and transport (distance traversed by wrist). A Markov analysis then examined the probabilistic effect of VF on which movement component exhibited higher variability over phases of the complete maneuver. Jerk-based metrics of smoothness (minimal jerk) and energy (integrated jerk-squared) were applied to indicate total movement efficiency with VF.

Results/Discussion—The reductions in grasp variability metrics with VF were significantly greater ($p<0.05$) compared to transport for velocity, acceleration, and jerk, suggesting separate control pathways for each component. The Markov analysis indicated that VF preferentially regulates grasp over transport when continuous control is modeled probabilistically during the movement. Efficiency measures demonstrated VF to be more integral for early motor planning of grasp than transport in producing greater increases in smoothness and trajectory adjustments (i.e., jerk-energy) early compared to late in the movement cycle.

Conclusions—These findings demonstrate the greater regulation by VF on kinematic performance of grasp compared to transport and how particular features of this relativistic control occur continually over the maneuver. Utilizing the advanced performance metrics presented in this

Correspondence: Zong-Ming Li, PhD, Cleveland Clinic, 9500 Euclid Avenue, ND20, Cleveland, OH 44195, Phone: (216) 444-1211, Fax: (216) 444-9198, liz4@ccf.org.

study facilitated characterization of VF effects continuously across the entire movement in corroborating the notion of separate control pathways for each component.

Keywords

reach; pinch; visual feedback; kinematics control

1 Introduction

The reach-to-grasp maneuver is commonly performed during activities of daily living. It requires coordination between the reaching hand and the involved grasping digits relative to the target object (Jeannerod 1981). For manipulation of smaller objects following reach, it is precision pinch grasp between the thumb and index finger that is utilized (Dubrowski, Bock et al. 2002). The composite reach-to-pinch function includes both global transport of the entire hand towards the object along with the opening and closing of the grasping digits upon the object. While the individual grasp and transport motion components are distinctly apparent, they are integrated into a single movement function (Coats, Bingham et al. 2008). There is debate as to what extent these individual components are independently regulated (Jeannerod 1984) versus the existence of more holistic control (Castiello, Bennett et al. 1998). Typically, assessments about presumed control structures were made according to discrete timing and kinematic features of the movements (e.g., time/amplitude of peak velocity, phase onset times, movement duration). While valid, these metrics only describe distinct cumulative features of the sensory-affected movement, such as feedback delays, but they do not necessarily indicate how control of kinematic performance is continuously regulated across the entire movement. Relative kinematic performance of these sub-movements under controlled provision of sensory feedback using metrics indicative of the continuous and whole- movement performance can serve to better indicate online sensory regulation by either singular versus separate control pathways.

The role of visual feedback has been extensively studied in reach-to-grasp performance to understand the interplay between the reach and grasp components, including effects of direction-dependence (Rossetti, Desmurget et al. 1995; van Beers, Sittig et al. 1999), integration with proprioception (Scheidt, Conditt et al. 2005), and selective visual perturbation of the target (Paulignan, Jeannerod et al. 1991; Paulignan, MacKenzie et al. 1991). These and other previous studies examining visual feedback have typically reported how kinematic hallmarks of the sub-movements are synchronized as evidence of mutual coordination. For example, it has been established that initiation of grasp closure is typically correlated with the onset of the deceleration phase of transport (Jeannerod 1984). Additionally, discrete changes in several transport and grasp component kinematic parameters can occur according to the level of visual feedback during the early phase of movement (Fukui and Inui 2006). Models have also been developed to demonstrate stereotypical kinematic features of reach-to-grasp to postulate their mode of control. These models include those coupling grip aperture and transport velocity (Hu, Osu et al. 2005), describing the temporal coordination of reach and grasp under optimal hand positioning (Hoff and Arbib 1993), and quantifying the contributions of vision and proprioception in position estimation for motor planning (Sober and Sabes 2003). As such, assessing the

dependence of readily evident kinematic parameters has provided insight into fundamental operating principles governing reach-to-pinch function. While vision-based paradigms have proven reliable in characterizing sensorimotor control previously, advanced performance metrics more comprehensively describing the reach-to-pinch movement are needed to establish control precepts of continuous online movement.

To this end, we formulated novel modes to assess vision-modulated kinematic performance for both the grasp and transport components across the entire reach-to-pinch movement. Such measures could suggest how the movement components are continually regulated with sensory feedback in indicating the existence of independent control pathways. Kinematic variability can signify the performance consistency of sub-movements and specify functional reliability with multiple repetitions of the task (Stergiou and Decker 2011). While motor variability may be inherent to biological systems and even functionally necessary for adaptations against transient perturbations (Davids 2006), increased variability still signifies decreased functional performance. Movement efficiency has classically been assessed using jerk-based measures to empirically evaluate smoothness of discrete movements such as reach-to-grasp (Hogan and Sternad 2007). Smoothness is indicative of skill and coordination since it is measured by minimizing jerk, which would otherwise entail greater motion fragmentation stemming from movement disorders (Rohrer, Fasoli et al. 2002). Therefore, jerk-based metrics may also be applied to examine the change of movement efficiency in response to particular sensory inputs or deficits. While variability and jerk-based metrics signify whole-movement performance, modeling performance probabilistically across its temporal phases demonstrates how movement components are relatively governed by sensory feedback on a continuous basis.

The primary objective of this study was to more comprehensively quantify the *continuous* and *whole-movement* performance of the grasping distal segments of the thumb and index finger in comparison to wrist transport during the reach-to-pinch movement with and without visual feedback of the reaching hand. In so doing, we can better understand the existence of independent versus coupled control pathways for grasp and transport on the basis of continuous online movement regulation. In generally evaluating comprehensive movement performance, we consider both movements occurring in three-dimensions (3-D) and examining movement across kinematic derivatives (position, velocity, acceleration, and jerk), since kinematic derivatives identify dynamic feedforward or feedback control adjustments (Jeannerod 1986). For more comprehensive examination specific to the *end-effector* for object manipulation during reach-to-pinch, both angular and linear kinematic efficiency of the distal segments (i.e., finger-pads) of the thumb and index finger needs to be considered. Endpoint (linear) variability of the thumb and index finger has been demonstrated to increase with rapid in-place grasp (Cole and Abbs 1986; Darling, Cole et al. 1988) and be a co-determinant of endpoint performance along with transport variability (Paulignan, Jeannerod et al. 1991). However, characterizing orientation (angular) has functional implications distinct and independent from endpoint position regarding grasp control of objects during and following the reach trajectory (Smeets and Brenner 2001; Lukos, Ansuini et al. 2007).

While removal of visual feedback of the reaching hand expectantly decreases movement performance, notable differentials in component performance supports the notion that grasp is uniquely regulated compared to transport and indicate the existence of independent control pathways as postulated by previous studies. Using this theoretical postulate, we apply our proposed variability and efficiency performance metrics to observe the presence of independent versus holistic control pathways for grasp and transport sub-movements based on continuous regulation across the entire reach-to-pinch maneuver. Confirmation of whether grasp and transport performance significantly differ relative to one another according to visual feedback condition based on comprehensive whole-movement metrics would strengthen the argument of independent pathways amongst the existing contrarian literature utilizing standard discrete metrics. Furthermore, confirmation based on the presented metrics would demonstrate sensory feedback control regulation occurring continuously across the entire movement in addition to singular effects such as creation of pure time-delays, changes in kinematic peak amplitudes, or variations in movement durations. The presented metrics for more comprehensive characterization of continuous whole-movement reach-to-pinch control include:

1. Trajectory variability metrics including movement-phase transition probabilities for a Hidden Markov Model (HMM). These metrics suggest the ability of visual feedback to reliably generate the entire sub-movement component and the probabilistic basis of which sub-movement requires relatively greater regulation across movement phases.
2. Jerk-based metrics (smoothness, jerk-energy) for characterizing whole-movement efficiency, which entails how well the movement is executed with sensory regulation.

The variability metrics are likely more indicative of online disruptions in feedback control regulation. Inability to robustly and consistently adapt according to new online sensory cues during the movement trajectory will contribute to increased trial-to-trial variability. Efficiency metrics may suggest deficits in either continual online feedback or preprogrammed feedforward control mechanisms. Less smooth movements may indicate an inaccurate pre-planned sensorimotor map in executing the movement. Higher jerk-energy profiles may suggest greater efforts to adapt the movement according to feedback for enacting a smoother motor plan for the remainder of the movement. Utilizing these metrics, we hypothesize that visual feedback will have the following effects on the reach-to-pinch maneuver:

1. Differing effects between grasp and transport, suggesting the existing of separate control pathways in continually regulating the entire maneuver
2. Greater effects on grasp relative to transport regarding variability, suggesting greater feedback regulation of grasp relative to transport by vision across the entire maneuver
3. Greater effects on grasp relative to transport regarding efficiency, suggesting greater feedforward (smoothness) and feedback adaptations (energy) across phases and the entire maneuver

4. Stabilizing the relative regulation of grasp versus transport probabilistically across phases and the entire maneuver

2 Methods

Subjects

Fifteen right-handed subjects were recruited to participate in this study. Only male subjects were tested to avoid gender-based differential effects. The mean age of the subjects was 31.1±4.9 years. These subjects had normal or corrected-to-normal vision and did not previously report nor demonstrate a history of disease, injury, or previous complications involving the hand and upper extremities. All subjects signed an informed consent approved by the local Institutional Review Board.

Collection of Marker Position Data for Digit Kinematics

Retro-reflective markers were affixed to the dorsal surface of the right hand of each subject. The 3-D position of each marker was tracked at 100Hz using a motion capture system (Model 460, Vicon® Motion Systems and Peak Performance, Inc., Oxford, UK). By experimental design, the reach-to-grasp fundamental movement frequency was relatively slow (specified at 1Hz). Therefore, sampling at 100Hz was sufficient for both capturing the motion and attaining adequate field of view for accurate tracking. A minimal marker set (Nataraj and Li 2013) was employed (Figure 1, TOP). To explicitly define the position and orientation of each distal digit segment, nail marker-clusters were employed with a digit alignment device (DAD) (Shen, Mondello et al. 2012). These nail marker-clusters were placed so the long-axis of the cluster stem was in-line with the central prominence of the finger-pad. To serve as a local reference to the hand, another “hand” marker-cluster was placed along the second metacarpal. Another marker (WR) was placed proximal to the wrist joint to track general transport of the hand. All 3-D marker position data were transformed to be expressed with respect to a “global” coordinate system affixed to the experiment platform-apparatus.

Computation of Finger-Pad Contact

Using each nail marker-cluster as a reference for a 3-D coordinate system, a spherical model of the respective digit finger-pad was represented (Figure 1, BOTTOM). A virtual “nail-point” is computed as a projection along the cluster stem to the dorsal surface of the nail and served as the center of the respective sphere. Using digital calipers, each digit thickness was measured as the transverse distance from dorsal surface to digit-pad prominence of the distal segment and served as the sphere radius. “Contact” between the thumb and index finger onto the target was assumed to occur according to two criteria: (1) the surfaces of the representative spheres for the two digits were separated by a distance equal to or less than 10 mm (i.e., the diameter of the marker target), and (2) the inter-distance velocity between the sphere centers was less than 15mm/sec. The distance between digit sphere surfaces is denoted as “inter-pad” distance.

Computation of Distal-Orientation-Coordination-Angle (DOCA)

Using the aligned 3-D coordinate system defined for each digit segment as described by (Shen, Mondello et al. 2012), angle rotations describing the relative orientation of the finger-pads were calculated as order-dependent (X-Y-Z) Euler angles as described in (Nataraj and Li 2013). These three Euler angle rotations represent the distal-orientation-coordination-angles (DOCA) of the distal thumb segment relative to the distal index finger segment and are denoted as Pitch-Yaw-Roll. The DOCA metric (orientation) along with nail-point (position) is necessary to fully characterize kinematics of the distal segments (i.e., end-effector) of the grasping digits.

Experimental Protocol

A custom platform-rig (Figure 2) was constructed to provide designated targets for performing the reach-to-pinch experiments with and without visual feedback of the reaching hand. The rig consisted of housing with a central slit to accommodate a high-resolution mirror (Imperial Glass & Door Company, Cleveland, OH) maintained in a vertical position. The mirror was 381mm high, 508mm deep, and 3.175 mm thick. With the mirror in place, the rig was divided into two alleys with the reflective side of the mirror facing the left alley. Each subject was seated facing the left alley containing a spherical marker-target (~10mm in diameter) placed 10cm high on a custom stand. The stand pole was designed to go through and 10cm higher than the target to visually discourage subjects from approaching the target from directly above. Subjects sat with head, body, and shoulders square to the left alley, and were asked to maintain consistent trunk and head posture during the subsequent reach-to-pinch trials. The subject was able to clearly gaze the mirror-reflection of the marker-target. Every subject was instructed to treat the marker reflection as the virtual target that could be physically contacted with the right hand following reach-to-pinch. The reflection was created to be 20cm directly in front of the starting position of the reaching right hand, which yielded comfortable reaching for all tested subjects. During reach-to-pinch trials with the mirror, there was no visual feedback (NVF) of the reaching hand since the subject's reaching right hand was behind the mirror in the right alley. Subjects also wore a head-strap with right-side blinder to further occlude any residual vision of movement cues from the reaching arm and shoulder. All subjects were able to be seated relative to the mirror-divide such that the mirror did not inhibit nor act as a barrier to reaching the virtual target. Given the high resolution of the mirror and subjects' maintaining steady head position, potential parallax effects should have been sufficiently mitigated.

For each reach-to-pinch trial, the experimenter asked the subject to be 'ready' prior to trial commencement, whereby the subject was seated correctly and placed the ulnar side of the right hand onto the designated starting area (towards platform corner) of the right alley with the thumb and index finger lightly in contact. Since the hand was not in view for NVF trials, the subject relied on tactile sensation to find the starting area, which had a clearly distinct texture. The three non-involved digits (middle, ring, and little fingers) were comfortably curled. To control for reach-to-pinch maneuver speed, every subject relied on an audio-metronome for movement cues. The audio-metronome produced moderate-pitch beeps at a frequency of 1Hz. To commence each trial, the experimenter provided an audible 'go' command, after which time, the subject self-selected which beep to commence the reach

with the right hand towards the virtual target. The subject paced the maneuver such that pinch contact was made approximately on the next (second) audible beep. To minimize dwell near contact, the subject immediately returned the hand to the starting position on the third beep to complete the trial. The subject was instructed to pinch the target with the thumb and index finger as accurately and consistently as possible. Following a few practice trials to accommodate to the procedure, a total of 40 consecutive NVF reach-to-pinch trials were executed with only a few seconds elapsing between trials according to experimenter discretion.

For the condition of visual feedback (VF) of the reaching hand during reach-to-pinch, the mirror was removed, and the real marker-target in the left-alley was moved to the right-alley such that it matched the location of the virtual target. The subject was again instructed to perform the reach-to-pinch maneuver as consistently as possible and at the metronome-specified pace. Again, after practice, another 40 consecutive reach-to-pinch trials were executed. For all subjects, the block of NVF trials was presented before the VF trials. This presentation of block-order ensured that subjects would not utilize proprioceptive memory (registered from positive tactile feedback from contacting real physical target) from the VF trials for the NVF trials. Standard randomized presentation of trial conditions would have otherwise facilitated subjects potentially relying on sensory memory for the NVF trials.

General Data Processing

The last 30 trials in each block for each subject were analyzed as the first 10 trials were treated as additional practice. The three-dimensional location of the virtual target was calculated using a series of transformations from a calibration trial as described in the “Appendix”. All data across all subjects were expressed with respect to a defined “pinch cycle” for each trial. The pinch cycle was defined to “start” when the inter-pad velocity first exceeded 15mm/sec and to “end” concurrently at finger-pad “contact”. These cycle definitions produced consistent and intuitive kinematic profiles for all subjects. Data for each pinch cycle trial was resampled to 100 points for subsequent data averaging to compensate for discrepancies in subjects exactly matching the metronome-pace. Derivatives were computed using the central finite-difference method:

$$x'(t_k)=\frac{x(t_{k+1})-x(t_{k-1})}{2\Delta t}$$

where $x(t_k)$, $x'(t_k)$ are the data value and the derivative value at t_k and Δt equals the sampling period (10ms). All data were then filtered using a third-order, low-pass Butterworth filter with cutoff at 20Hz. The aforementioned data processing was performed on the following measured variables for grasp and transport:

1. Inter-pad distance (*grasp-linear*) = distance between sphere-model surfaces of finger-pads
2. DOCA (*grasp-angular*) = relative orientation of aligned coordinate systems affixed to thumb finger-pad relative to that of index finger

3. Wrist path-length (*transport*) = 3-D path-length distance traversed by wrist marker from initial position (i.e., from "start" of reach-to-pinch movement cycle)

Kinematic Performance Metrics

For the grasp and transport variables identified, the following movement performance quantities were tabulated across subjects for each visual condition:

1. "Trajectory variability" was represented by the trial-to-trial standard deviation about the mean trajectory across the pinch cycle. Trajectory variability signifies reliable performance control for a continually modifiable movement (Flanagan, Ostry et al. 1993).
2. Jerk-based efficiency metrics:
   a. "Smoothness" of each trajectory across the entire movement cycle was computed by the normalized integrated jerk function from (Hogan and Sternad 2009):

$$\text{Smoothness}=\frac{\left(\int_{t_1}^{t_2} \dddot{x}\,(t)^2 dt\right) D^5}{A^2}$$

   where A is the trajectory amplitude/extent and D is the duration ($t_2 - t_1$).

   b. "Phase Energy" of the jerk signal across a given phase (t_{start} to t) within the cycle:

$$E(t)=\int_{t_{start}}^{t} |j(t)|^2 dt$$

   where t = pinch cycle time, E = time-cumulative jerk energy, and $j(t)$ = variable jerk-value over time. This energy function is similar to the smoothness criterion from (Hogan and Sternad 2007).

The energy metric served two purposes. First, it was used to identify three phases (early, middle, late) within the movement cycle since a reaching movement is known to have initial acceleration to fast-velocity, steady transport, and terminal deceleration to low-velocity components (Jeannerod 1984; Fukui and Inui 2006). Second, distinct profiles in jerk energy may signify the effects of visual feedback in distinctly coordinating the actions of grasp versus transport. For example, notably jerky motions made early compared to late in the movement may signify early motor planning to ensure smoother movement termination.

Jerk-energy is natural for phase identification since a distinctly smooth "middle" phase may exist during steady transport or kinematic pause (e.g., near maximum grasp aperture), which is unique from phases containing rapid rates of change (e.g., movement initiation and termination). Following application of a moving average (window equals 1/3 the pinch cycle) to $E(t)$, the middle-phase was identified as the signal portion with slope < 10% the maximum slope observed. This portion was a stereotypical feature observed for all subjects.

The two remaining signal portions before and after the middle phase were designated the "early" and "late" phases, respectively.

Markov Analysis

To examine the online *relative interactions* between grasp and transport variability across the pinch cycle, additional 3-D variability sequences for grasp and transport were constructed and modeled as probabilistic Markov processes. Each sequence was composed of 100 points corresponding to the 100 sampling instances across the pinch cycle. For grasp variability, the 3-D position coordinates of the computed nail-point for thumb and index finger were utilized and underwent the aforementioned data processing. For transport variability, the 3-D coordinates of the wrist marker were utilized and processed accordingly. The grasp sequence was defined as the norm of the 3-D trajectory variability for the thumb nail-point summed with that of the index finger. To observe grasp variability empirically-independent from transport, grasp variability was expressed with respect to the "local" hand coordinate system. The transport sequence was defined as the norm of the 3-D trajectory variability for the wrist marker expressed in the "global" platform coordinate system per usual. To compare grasp and transport sequences on the same scale, each sequence was normalized by its own maximum. Another sequence was created with each point represented by a 2-component unit-vector whose original components were the corresponding values from the grasp and transport sequences. To observe the *relative* variability between grasp and transport, the 2-component unit-vector was converted to an equivalent polar angle (x-axis = transport, y-axis = grasp) restricted to be between 0° and 90° since normalized variability values were constrained over [0,1]. This polar angle was designated as the relative variability angle (θ) across the pinch cycle, and θ was computed for NVF and VF conditions.

A hidden Markov model was utilized in assuming that the states are unobserved (hidden) and that the observed "emission" sequence is which "phase" (early, middle, or late) of the pinch cycle is currently observed (Bishop 2006). The state sequence of the Markov model, as seen in Figure 3, were defined according to which variability component (grasp, transport) was relatively greater: (1) Transport>Grasp (i.e., $\theta<45°$); (2) Grasp>Transport(i.e., $\theta>45°$)). Specifying state and emission sequences in this manner facilitates identification of whether grasp or transport variability dominates over the movement cycle. The Markov state-state transition and state-emission probabilities for the given state, emission sequences were estimated using the 'hmmestimate' function in MATLAB®. The function provides a probabilistic model represented by maximum likelihood estimators for the transition and emission values given the data sequences supplied.

Statistical Analysis

For each subject, data was averaged across all trials per visual condition (VF, NVF) to provide the mean values for that subject and condition. Normal distributions were not observed for several parameters based on the Kolmogorov-Smirnov and Shapiro-Wilk tests for normality. As such, non-parametric statistical hypothesis testing was applied to make comparisons without assuming normality. Specifically, the Wilcoxon signed-rank test was employed to compare significant differences between NVF and VF ($p<0.05$).

3 Results

The kinematic performance metric of trajectory variability for grasp (inter-pad distance, DOCA) and transport (wrist path-length) variables and their 1st (velocity), 2nd (acceleration), and 3rd (jerk) derivatives across the pinch cycle are visualized in Figure 4. The variability is represented by the standard deviation bands (dotted lines) about the respective mean trajectories (solid lines) across all subjects. Trajectories for inter-pad distance and wrist path-length demonstrate two and one distinct movement components, respectively. Inter-pad distance demonstrates the thumb and index finger digits initially together (closed) prior to maximum aperture (wide-open) before returning the two digits back together (closed) upon the presumed contact target. Wrist path-length generally represents movement of the entire hand away from its starting position to the target. As such, the derivatives for inter-pad distance exhibit biphasic transitions for both the initiation and termination of the reach-to-pinch maneuver. Typically, the standard deviation bands are greatest during these transitions and are notably pronounced with NVF. Similar trends are observed with DOCA as the standard deviation bands with NVF demonstrate bursting at these transitions.

The trajectory variability results for each visual condition, the percentage differentials between visual conditions, and whether the differential was greater for grasp versus transport are summarized in Table 1A. With VF, variability was significantly reduced ($p<0.05$) for all presented variables. For DOCA, only the pitch component is presented since significant differences were not observed for yaw or roll ($p>0.05$). When comparing the percentage reduction in variability with VF between grasp and transport variables, the reductions were significantly greater on grasp for velocity, acceleration, and jerk ($p<0.05$). The kinematic performance quantity results of movement smoothness for these selected grasp and transport variables (Table 1B) were significantly increased with VF ($p<0.05$). However, in comparing these smoothness increases between grasp and transport variables, these differences were not significant ($p>0.05$).

Figure 5 shows a representative subject mean trajectory for inter-pad (grasp, TOP) and wrist path-length (transport, BOTTOM) jerk outcomes along with the corresponding jerk-energy signal, phases, and cumulative energy binned at each phase as displayed by the respective area-fills. The lowest energy for grasp is during the middle phase for both VF and NVF conditions as shown in Table 1C. Grasp energy across all three phases was higher for NVF but only significantly for the early and late phases ($p<0.05$). The mean ratio of early-to-late phase energy with VF (mean across all subjects equals 18.7) was significantly greater than that with NVF (mean equals 3.5) at $p=0.05$.

Transport did not include a distinct intermediate pause as with grasp, and a distinct low-energy middle phase unique to transport was not similarly identified. So, the displayed energy bins for transport correspond to those identified for grasp. Differences in transport energy between NVF and VF were not significant for any of the three phases ($p>0.05$). Furthermore, the ratio of early-to-late phase energy was also not significant between visual conditions ($p>0.05$). However, the magnitude and direction of the percentage change in

early-to-late energy with visual feedback for grasp (+434%) versus transport (−43%) was significantly evident ($p<0.001$).

Sample Markov state-sequence paths represented by mean relative variability angles over the pinch cycle for kinematic derivatives of a representative subject are shown in Figure 6. Depending on the kinematic derivative or visual feedback condition, unique circuitous paths were observed. Across all kinematic data, the mean path-length for the unwrapped data was significantly greater for NVF (89.5±18.2°) than VF (79.3±20.7°) at $p=0.01$ (z-value=−3.17).

To assess whether the circuitous variability paths had systematic probabilistic features moving between states of higher transport (State 1) versus higher grasp (State 2) variability, the Markov state transition and emission probabilities were tabulated in Tables 2 and 3, respectively. As seen in Table 2, there are generally large (>80%) self-state transitions probabilities, which indicates the strong tendency to remain in a state already assumed. Across visual conditions, significant differences in self-state transition probability only existed with position kinematics where for NVF State 1 and State 2 probabilities were higher and lower than VF, respectively. However, the linear trend (from position to jerk) in self-state probability for both states across kinematic derivatives were significantly different for both state across visual conditions. The self-state probability signficantly ($p<0.05$) trended towards decrease for both states with greater decrease magnitude for NVF than VF for both states. The emission probabilities listed in Table 3 indicate the probability each state is associated with a particular phase (i.e., early, middle, late). No differences across visual condition was observed, however the linear trends across derivatives were significant ($p<0.05$). The largest trends (slope>0.05) were observed with the early and late phase trends for State 1.

4 Discussion

The present study investigates the effects of visual feedback on the grasping digits relative to hand transport to examine the notion of independent versus separate control mechanisms for grasp and transport using comprehensive kinematic performance metrics that holistically describe control across the entire reach-to-pinch maneuver. These metrics for improved performance included reduction in trajectory variability, increase in movement smoothness, and higher early-to-late phase energy. A Markov analysis was performed to examine how visual feedback may be probabilistically regulating relative variability of grasp versus transport across the phases of the reach-to-pinch movement. The selected performance metrics not only demonstrate the intrinsic value of visual feedback in coordinating performance of the reach-to-pinch maneuver, but they also parse out the relative effects of visual feedback on the linear *and* angular grasp components versus transport on the basis of continual regulation across the entire maneuver. By examining the problem in this manner, it becomes observable if the effects of visual feedback on grasp and transport are indeed differently predicated on persistent control. If so, we can further refute or corroborate the notion that separate pathways for sensorimotor control of grasp versus transport may exist beyond classic metrics utilizing discrete descriptors of kinematic features which mainly identify distinct transient and amplitude effects.

While kinematic performance of both the grasp and transport components were compromised without visual feedback, the relatively greater effect on grasp suggests not only the elevated role of visual feedback in regulation of the digits but also a dedicated control pathway for grasp. Holistic control of grasp and transport would suggest that the relative effects upon kinematic performance across both components would be similar. This notion supports likewise conclusions of separate, but coordinated, control mechanisms by previous studies utilizing metrics describing kinematic synchrony between grasp and transport (Jeannerod 1984; Paulignan, MacKenzie et al. 1991; Dubrowski, Bock et al. 2002). Those studies examined correlation in timing or differences in kinematic variability at discrete portions of the reach-to-grasp movement. In this study, performance metrics across kinematic derivatives and the entire movement cycle were examined to comprehensively assess the effects of visual feedback on movement efficiency of each component in discerning independent control mechanisms.

Kinematic Performance

For all reported variables characterizing grasp (inter-pad distance, DOCA-Pitch) and transport (wrist path-length), removal of visual feedback of the reaching hand expectantly increased variability and reduced smoothness of the position trajectory. In the case of grasp angle (DOCA), all three angular degrees-of-freedom were measurable and characterized, but only Pitch showed a significant difference across visual conditions. Since Euler angles were computed in the Pitch-Yaw-Roll order, Pitch was the angular degree-of-freedom assumed to contribute most to grasp orientation. Despite how the angle measurements are projected, there appears to be a significant performance difference with VF in the angular dimension. However, this performance differential in grasp angle was not significantly greater than transport. This suggests that variability of distal-segment orientation may not be necessarily regulated more by visual feedback than transport. But since grasp angle can be varied independently of grasp position (e.g., inter-pad distance) and may exhibit unique control elements(Lukos, Ansuini et al. 2007), making the distinction between grasp angle and linear-position an important consideration.

The relatively greater reductions in movement performance without visual feedback for grasp in the linear-position dimension compared to transport were significant in terms of inter-pad distance trajectory variability at the velocity, acceleration, and jerk derivative levels. This suggests that it is control of grasp linear-position, rather than grasp orientation, with hierarchical precedence over transport in control of the maneuver by visual feedback. As such, visual feedback may be more necessary to independently regulate changes (derivatives) in grasp inter-pad distance, while grasp orientation may be more coupled with the control pathway regulating gross hand transport. However, the apparent greater dependence on visual feedback for improved kinematic performance of linear grasp, in terms of reduced variability, compared to transport still suggests existence of independent control pathways. However, in this study, we have demonstrated a distinction in control pathways for linear and angular grasp control such that grasp orientation either is not as well regulated as grasp endpoint position or possibly has greater coupling with the transport pathway.

While visual feedback significantly improved movement smoothness for all observed grasp and transport variables, relative improvement for grasp smoothness was not significantly greater than for transport. Therefore, it appears that sensitive differences in visual feedback regulation of these movement components are better reflected in the derivatives of trajectory variability than movement smoothness. This re-implicates the role of visual feedback in more greatly regulating online *dynamic* changes in grasp compared to transport as opposed to pre-planning the enacted feedforward control of the maneuver prior to movement initiation.

Jerk Energy for Pinch Phase Identification

In using jerk-energy of grasp (inter-pad distance) as the reference for identifying phases of the reach-to-pinch movement, it was clearly observed that greater grasp energy was expended early relative to late in the movement with visual feedback present. Using these same phase definitions, the difference in early-to-late jerk-energy ratio for transport (wrist path-length) with visual feedback was not significant. Taken together, it further implicates the distinct effect of visual feedback in temporal regulation of grasp over transport as grasp may employ greater early-phase motor adjustments after the movement is initiated for successful movement execution.

Distinct early- and late- phases for the reach-to-grasp maneuver have been previously identified according to respective fast- and slow-velocity profiles (Jeannerod 1984), and it has been classically suggested that the initial phase is governed primarily by feedforward motor planning (Wolpert and Miall 1996). Over the course of the movement, and especially at convergence for precise endpoint positioning, a feedback mode may take control for adaptive corrections (Milner 1992). Our energy analysis suggests that notable adjustments are being made early in the maneuver cycle with VF for grasp to allow for more efficient convergence of the digits upon the endpoint. This corroborates notions of visual feedback being critical for both planning (Desmurget, Pelisson et al. 1998) and producing synergistic patterns according to online sensory cues (Santello, Flanders et al. 2002). This also supports findings from (Fukui and Inui 2006), indicating the critical value of online vision during the early phase of prehensile motion. However, our finding makes a clear distinction in utilization of visual feedback for planning and early-movement adjustments being more profound for grasp than general hand transport based on energy-metrics which more comprehensively described motor actions occurring cumulatively across the major phases of the movement.

Regulation of Grasp and Transport Variability States

We applied the hidden Markov model to examine how visual feedback actively provided a probabilistically stabilizing influence in the relative regulation of grasp versus transport variability across the pinch cycle. We first demonstrated the general increase in variability for both grasp and transport without visual feedback with that for grasp being relatively greater. However, with the Markov model we demonstrate that this greater relative variability of grasp over transport is also continually regulated by visual feedback in distinct ways. First, shorter relative variability angle traces with visual feedback indicate that visual feedback acts to better fix, or stabilize, this relative variability over the maneuver. Second,

generally higher self-state variability values for state 2 compared to state 1 demonstrates the continual tendency to move towards a higher grasp variability state. Third, and finally, this regulation is persistent across the movement since distinct differences in control shifting between movement phases (i.e., early, middle, late) were not apparent.

For the relative variability angle trace used for the Markov state sequence, the shorter-path length observed for VF demonstrated that visual feedback minimized shifts in relative variability between transport and grasp across the pinch cycle. The shorter path-length also indicates grasp and transport variability shifting more synchronously over the pinch cycle. From this observation, it may be inferred that visual feedback is necessary to better couple control of the grasping digits with that of hand transport. Therefore, while separate control pathways for grasp and transport may exist, deficit in visual feedback may produce disruption in coordinating the synergy across these sub-movement components.

The hidden Markov model itself was utilized to determine the probability of remaining in a particular variability state (i.e., relatively high transport variability versus high grasp variability) across pinch cycle phases for each visual condition. Although the difference in self-state transition probabilities across visual conditions was only significant at the position level, the rate of probabilistic change (i.e., linear slope) across kinematic derivatives was significant and significantly different across visual conditions. This observation demonstrates the distinct shift in relative online regulation of variability between grasp and transport depending on visual feedback. Furthermore, the lower self-state probability with higher kinematic derivatives for state 1 compared to state 2 implies the tendency for more required control of grasp compared to transport. The slope-trends being significantly lower for VF than NVF also demonstrates the role of vision in reducing transitions between variability states thereby more effectively regulating the entire movement.

The Markov probabilities for associating phase with a particular variability state (emission outputs) did not exhibit significant differences in probabilities or trends across visual conditions. This finding suggests that while visual feedback may regulate grasp and transport, the relative governance between components may not be phase-dependent. For both visual conditions, there was a noteworthy reciprocal effect whereby state 1 demonstrated low-to-high “early” emission probability across kinematic derivatives specifically balanced against high-to-low “late” emission probability. This may indicate a tendency towards greater dynamic adaptations being needed for the transport component across the movement regardless of visual feedback.

Summary and Future Considerations

Examining the kinematic effects of visual feedback to understand the interplay between grasp and transport illuminates possible underlying motor control primitives for the reach-to-pinch maneuver. These primitives include correlating goal-directed sub-movements to feedforward and feedback control mechanisms (Jeannerod 1984; Flanagan, Ostry et al. 1993), postulates for motor planning (Desmurget and Grafton 2000), and identifying kinematic parameters for movement control objectives (Meyer, Abrams et al. 1988), and transient changes in kinematic profiles that signify movement adaptations continually responding to online performance (Darling, Cole et al. 1988; Sartori, Straulino et al. 2011).

In this study, we employed kinematic performance metrics that demonstrate relativistic motor regulation by visual feedback of transport versus grasp as a more comprehensive function of the entire reach-to-pinch maneuver. While visual feedback expectantly improved kinematic performance of both components in terms of reduced trajectory variability, increased smoothness, and higher early-to-late jerk-energy, the effects on each component were significantly different. Therefore, while visual feedback appears generally indispensable for reliable functional performance, the notable differences in relativistic effects on grasp versus transport suggest that visual feedback regulates grasping digit kinematics separately from that of general hand transport and on a continual basis. It is possible that the digit kinematics function according to biomechanical features of the grasping digits (Gentilucci, Roy et al. 2004). In which case, visual feedback may provide necessary dynamic updates of the system states of the digits relative to the target for high-level performance.

Visual feedback appears to be integral for both early-motor planning in coordinating grasp and final convergence of the digits upon the target. Accuracy for complex multi-joint tasks require updating the representation of limb mechanical properties (Lacquaniti 1992). As with the movement planning for the reaching limb (Ghez, Gordon et al. 1995), our results suggest that vision may serve as the feedback necessary to continually update the system representation, including dynamic properties, for movement planning of the grasping digits. Thus, as with integrated spatial coding for the hand and digits for tactile stimuli (Heed, Backhaus et al. 2012) or sensorimotor encoding between visual feedback and the reaching limb (Scheidt, Conditt et al. 2005), similar computational models quantifying visual effects, including movement planning, upon the grasping digits may be formulated in the future utilizing the presented movement metrics of this study.

Examining the dependence on vision for accurate functional manipulation of the thumb and index finger also has important implications for potentially characterizing sensorimotor deficit. Future investigations may study the effects of visual feedback on the digits for individuals with compromised sensory capabilities. To further identify the physiological substrate for neuromotor control of the reach-to-pinch movement, the effects of visual feedback in the presence of pathologies that incite sensorimotor dysfunction upon the digits, such us carpal tunnel syndrome (Lowe and Freivalds 1999), should be investigated. Quantifying the reliance on vision for reach-to-pinch maneuvers may facilitate the assessment of deficit due to central- or peripheral-level disorder. Specifically, individuals afflicted with such sensorimotor deficit may have made functional adaptations to rely on alternative sensory modalities (e.g. visual) as compensation (Ghez, Gordon et al. 1995). When investigating the sensorimotor effects of particular pathologies, it may also be of interest to examine *endpoint* (i.e., 3-D contact point between digits) variability between subject groups for the NVF case. This experimental paradigm would test fundamental proprioceptive capabilities in localizing the digits about the perceived target. In this case, partitioning the proportion of endpoint variability resulting from variability accrued during the motion may be warranted to isolate true endpoint variability.

Acknowledgments

This study was supported by Grant Number R01AR056964 from NIAMS/NIH.

References

Bishop, C. Pattern Recognition and Machine Learning. New York: Springer; 2006.

Castiello U, Bennett K, et al. Reach to grasp: the response to a simultaneous perturbation of object position and size. Experimental brain research Experimentelle Hirnforschung Experimentation cerebrale. 1998; 120(1):31–40.

Coats R, Bingham GP, et al. Calibrating grasp size and reach distance: interactions reveal integral organization of reaching-to-grasp movements. Experimental brain research Experimentelle Hirnforschung Experimentation cerebrale. 2008; 189(2):211–220.

Cole KJ, Abbs JH. Coordination of three-joint digit movements for rapid finger-thumb grasp. Journal of neurophysiology. 1986; 55(6):1407–1423. [PubMed: 3734863]

Darling WG, Cole KJ, et al. Kinematic variability of grasp movements as a function of practice and movement speed. Experimental brain research Experimentelle Hirnforschung Experimentation cerebrale. 1988; 73(2):225–235.

Davids, KBS.; Newell, K. Movement System Variability. Champaign, IL: Human Kinetics; 2006.

Desmurget M, Grafton S. Forward modeling allows feedback control for fast reaching movements. Trends in cognitive sciences. 2000; 4(11):423–431. [PubMed: 11058820]

Desmurget M, Pelisson D, et al. From eye to hand: planning goal-directed movements. Neuroscience and biobehavioral reviews. 1998; 22(6):761–788. [PubMed: 9809311]

Dubrowski A, Bock O, et al. The coordination of hand transport and grasp formation during single- and double-perturbed human prehension movements. Experimental Brain Research. 2002; 145(3): 365–371. [PubMed: 12136386]

Flanagan JR, Ostry DJ, et al. Control of Trajectory Modifications in Target-Directed Reaching. Journal of motor behavior. 1993; 25(3):140–152. [PubMed: 12581985]

Fukui T, Inui T. The effect of viewing the moving limb and target object during the early phase of movement on the online control of grasping. Human Movement Science. 2006; 25(3):349–371. [PubMed: 16707178]

Gentilucci M, Roy AC, et al. Grasping an object naturally or with a tool: are these tasks guided by a common motor representation? Experimental brain research Experimentelle Hirnforschung Experimentation cerebrale. 2004; 157(4):496–506.

Ghez C, Gordon J, et al. Impairments of reaching movements in patients without proprioception. II. Effects of visual information on accuracy. Journal of neurophysiology. 1995; 73(1):361–372. [PubMed: 7714578]

Heed T, Backhaus J, et al. Integration of hand and finger location in external spatial coordinates for tactile localization. Journal of experimental psychology Human perception and performance. 2012; 38(2):386–401. [PubMed: 21688947]

Hoff B, Arbib MA. Models of Trajectory Formation and Temporal Interaction of Reach and Grasp. Journal of motor behavior. 1993; 25(3):175–192. [PubMed: 12581988]

Hogan N, Sternad D. On rhythmic and discrete movements: reflections, definitions and implications for motor control. Experimental Brain Research. 2007; 181(1):13–30. [PubMed: 17530234]

Hogan N, Sternad D. Sensitivity of smoothness measures to movement duration, amplitude, and arrests. Journal of motor behavior. 2009; 41(6):529–534. [PubMed: 19892658]

Hu Y, Osu R, et al. A model of the coupling between grip aperture and hand transport during human prehension. Experimental brain research Experimentelle Hirnforschung Experimentation cerebrale. 2005; 167(2):301–304.

Jeannerod, M. Intersegmental coordination during reaching at natural visual objects. In: Long, JAB., editor. Attention and Performance IX. Hillsdale, NJ: Erlbaum; 1981. p. 153-169.

Jeannerod M. The timing of natural prehension movements. Journal of motor behavior. 1984; 16(3): 235–254. [PubMed: 15151851]

Jeannerod M. Mechanisms of visuomotor coordination: a study in normal and brain-damaged subjects. Neuropsychologia. 1986; 24(1):41–78. [PubMed: 3517680]

Lacquaniti F. Automatic control of limb movement and posture. Current opinion in neurobiology. 1992; 2(6):807–814. [PubMed: 1477544]

Lowe BD, Freivalds A. Effect of carpal tunnel syndrome on grip force coordination on hand tools. Ergonomics. 1999; 42(4):550–564. [PubMed: 10204420]

Lukos J, Ansuini C, et al. Choice of contact points during multidigit grasping: effect of predictability of object center of mass location. The Journal of neuroscience : the official journal of the Society for Neuroscience. 2007; 27(14):3894–3903. [PubMed: 17409254]

Meyer DE, Abrams RA, et al. Optimality in human motor performance: ideal control of rapid aimed movements. Psychol Rev. 1988; 95(3):340–370. [PubMed: 3406245]

Milner TE. A model for the generation of movements requiring endpoint precision. Neuroscience. 1992; 49(2):487–496. [PubMed: 1436478]

Nataraj R, Li ZM. Robust identification of three-dimensional thumb and index finger kinematics with a minimal set of markers. Journal of biomechanical engineering. 2013; 135(9):91002–91009. [PubMed: 23775305]

Paulignan Y, Jeannerod M, et al. Selective perturbation of visual input during prehension movements. 2. The effects of changing object size. Experimental brain research Experimentelle Hirnforschung Experimentation cerebrale. 1991; 87(2):407–420.

Paulignan Y, MacKenzie C, et al. Selective perturbation of visual input during prehension movements. 1. The effects of changing object position. Experimental brain research Experimentelle Hirnforschung Experimentation cerebrale. 1991; 83(3):502–512.

Rohrer B, Fasoli S, et al. Movement smoothness changes during stroke recovery. The Journal of neuroscience : the official journal of the Society for Neuroscience. 2002; 22(18):8297–8304. [PubMed: 12223584]

Rossetti Y, Desmurget M, et al. Vectorial coding of movement: vision, proprioception, or both? Journal of neurophysiology. 1995; 74(1):457–463. [PubMed: 7472347]

Santello M, Flanders M, et al. Patterns of hand motion during grasping and the influence of sensory guidance. The Journal of neuroscience : the official journal of the Society for Neuroscience. 2002; 22(4):1426–1435. [PubMed: 11850469]

Sartori L, Straulino E, et al. How objects are grasped: the interplay between affordances and end-goals. PloS one. 2011; 6(9):e25203. [PubMed: 21980396]

Scheidt RA, Conditt MA, et al. Interaction of visual and proprioceptive feedback during adaptation of human reaching movements. Journal of neurophysiology. 2005; 93(6):3200–3213. [PubMed: 15659526]

Shen ZL, Mondello TA, et al. A digit alignment device for kinematic analysis of the thumb and index finger. Gait & posture. 2012; 36(3):643–645. [PubMed: 22633016]

Smeets JB, Brenner E. Independent movements of the digits in grasping. Experimental brain research Experimentelle Hirnforschung Experimentation cerebrale. 2001; 139(1):92–100.

Sober SJ, Sabes PN. Multisensory integration during motor planning. The Journal of neuroscience : the official journal of the Society for Neuroscience. 2003; 23(18):6982–6992. [PubMed: 12904459]

Stergiou N, Decker LM. Human movement variability, nonlinear dynamics, and pathology: is there a connection? Human Movement Science. 2011; 30(5):869–888. [PubMed: 21802756]

van Beers RJ, Sittig AC, et al. Integration of proprioceptive and visual position-information: An experimentally supported model. Journal of neurophysiology. 1999; 81(3):1355–1364. [PubMed: 10085361]

Wolpert DM, Miall RC. Forward Models for Physiological Motor Control. Neural networks : the official journal of the International Neural Network Society. 1996; 9(8):1265–1279. [PubMed: 12662535]

- We examined the effect of visual feedback of the hand on performance of the reach-to-pinch function
- Visual feedback reduced variability and improved smoothness of the reach-to-pinch movement
- Visual feedback appears to play a relatively greater role in regulating grasp compared to transport
- The results of this study suggest that separate control pathways exist for grasp and transport

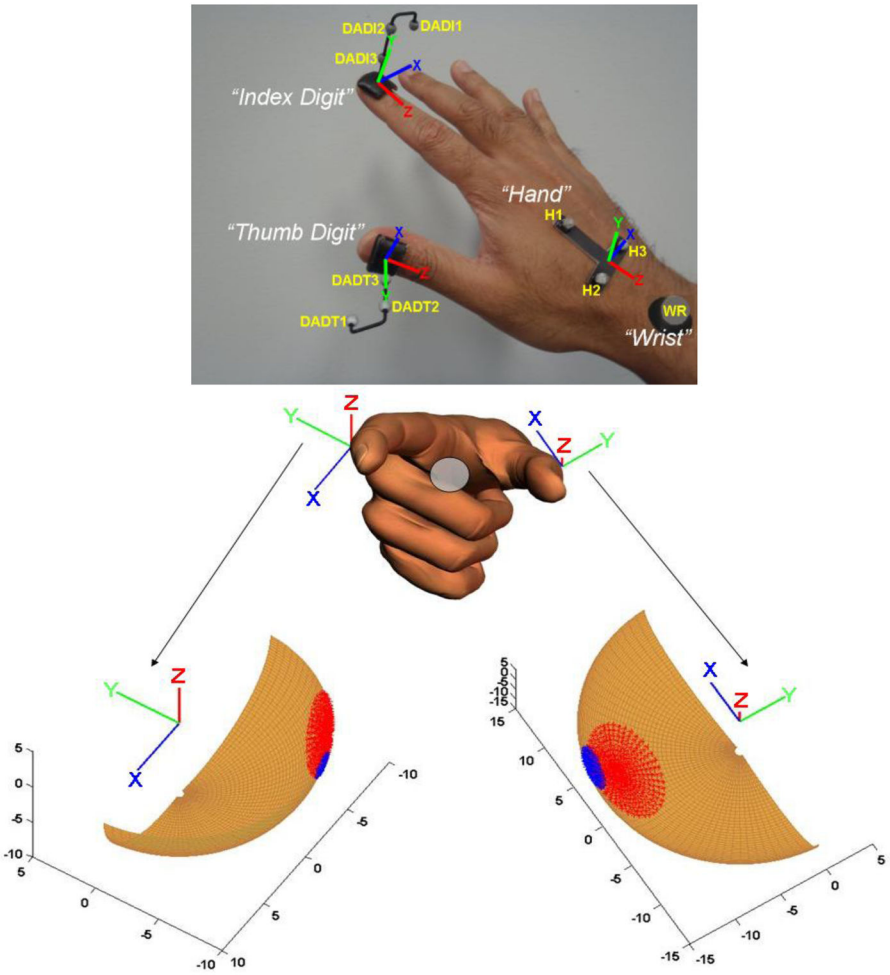

Figure 1.

TOP: Marker set included nail marker-clusters on distal segments of the thumb and index finger, hand marker-cluster along the second metacarpal, and single marker proximal to wrist. Anatomically-aligned X-Y-Z coordinate systems also shown for marker-clusters.

BOTTOM: Representative spherical models (units in 'mm') of digit-pads used to estimate 'contact' onto marker-target (gray transparent sphere). Coordinate systems for digits have origin at "nail-point".

Note: Circular areas on digit-pads depict example mean contact areas for VF (blue) and NVF (red) conditions.

Note: Euler angle rotations of the aligned X-Y-Z coordinate system of the thumb relative to the index finger represent the distal-orientation-coordination-angle (DOCA)

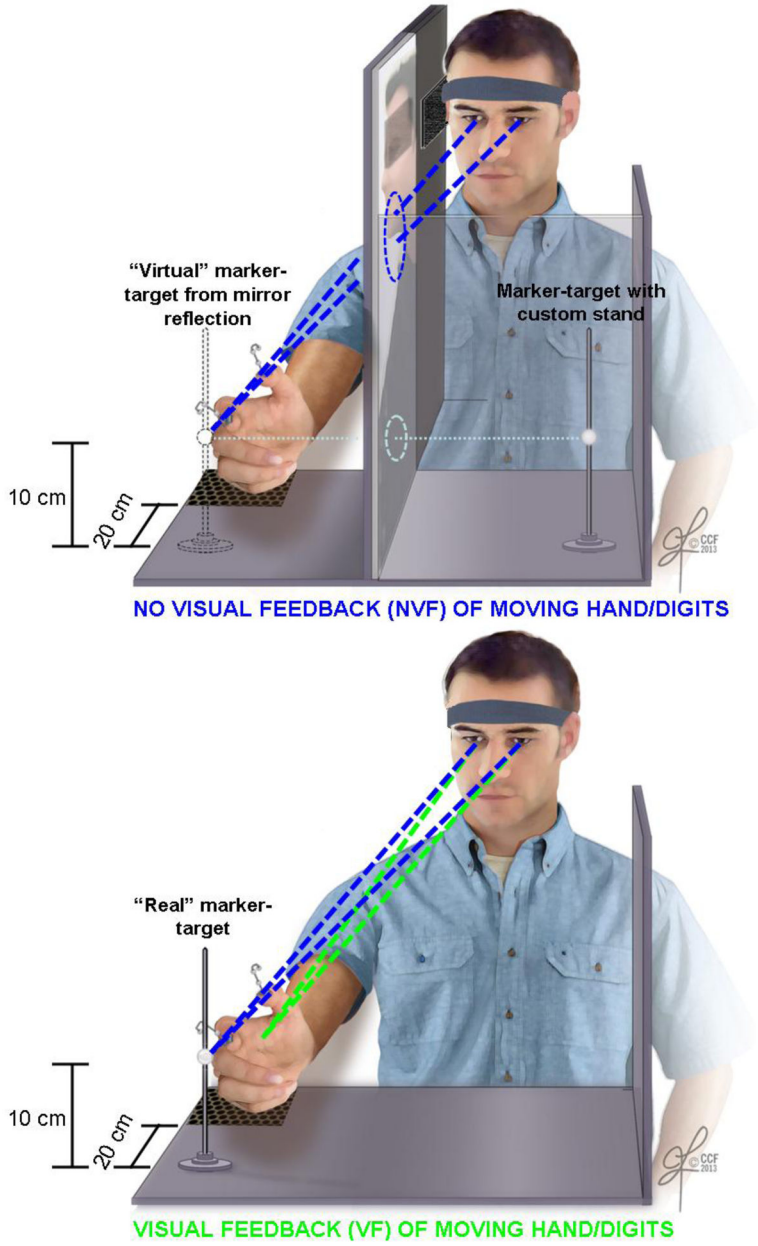

Figure 2.

Two experimental conditions using custom platform-rig. TOP: Condition where subject has no visual feedback (NVF) of moving hand and grasping digits but still views "virtual" marker-target in 3-D space from mirror reflection. BOTTOM: Subject has visual feedback (VF) of hand, grasping digits, in directly contacting "real" marker-target.

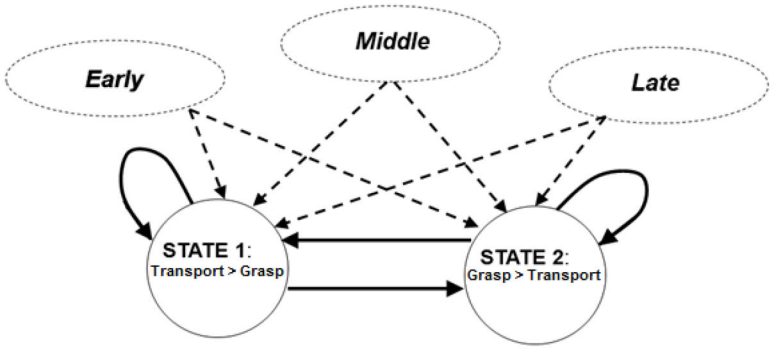

Figure 3.

State diagram for Hidden Markov Model showing state-state transitions by solid arrow lines and emission observations (early, middle, late) associated with each state shown by dotted lines.

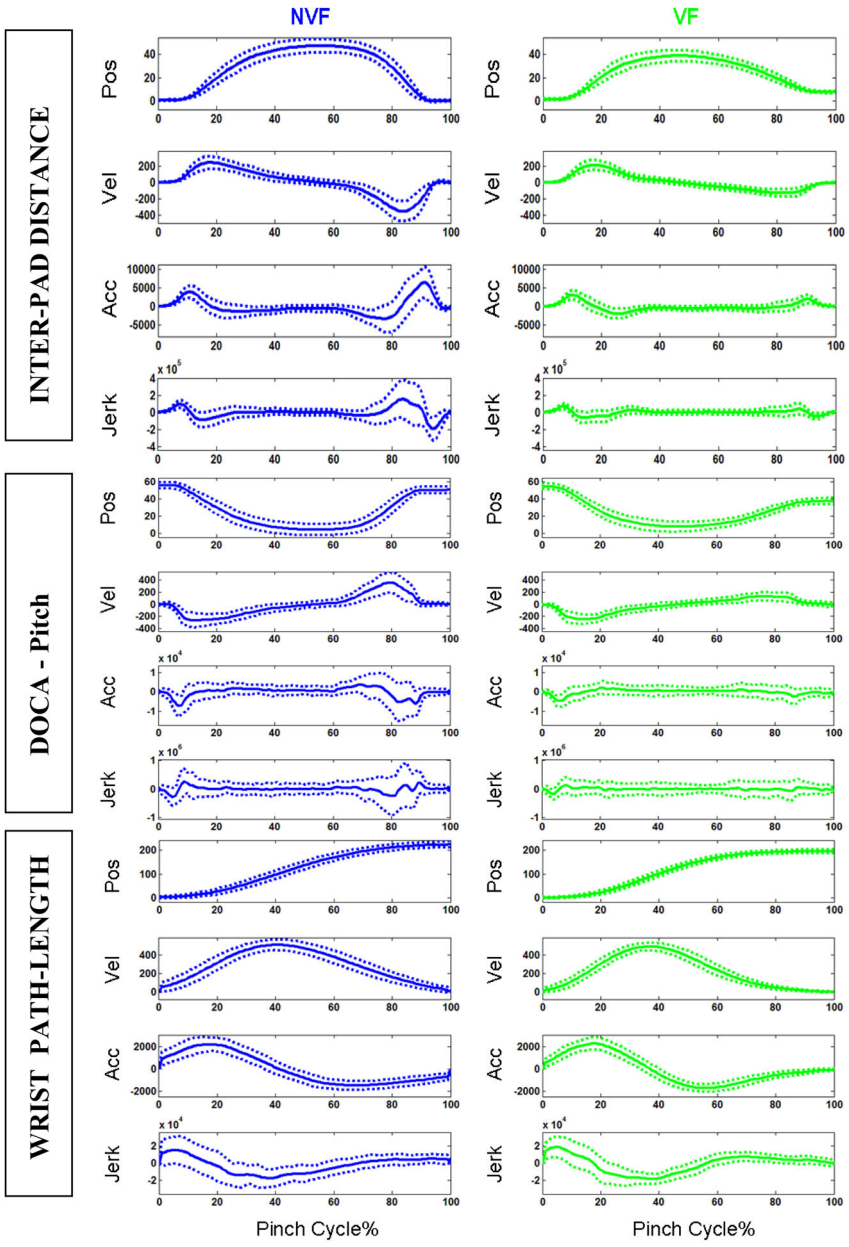

Figure 4.

Mean (solid line) position, velocity, acceleration, and jerk trajectories across all subjects for inter-pad distance, DOCA-pitch, and wrist path-length with no visual feedback (NVF, left) of hand and with visual feedback (VF, right).

Note: +/− standard deviation (variability) represented by dotted lines.

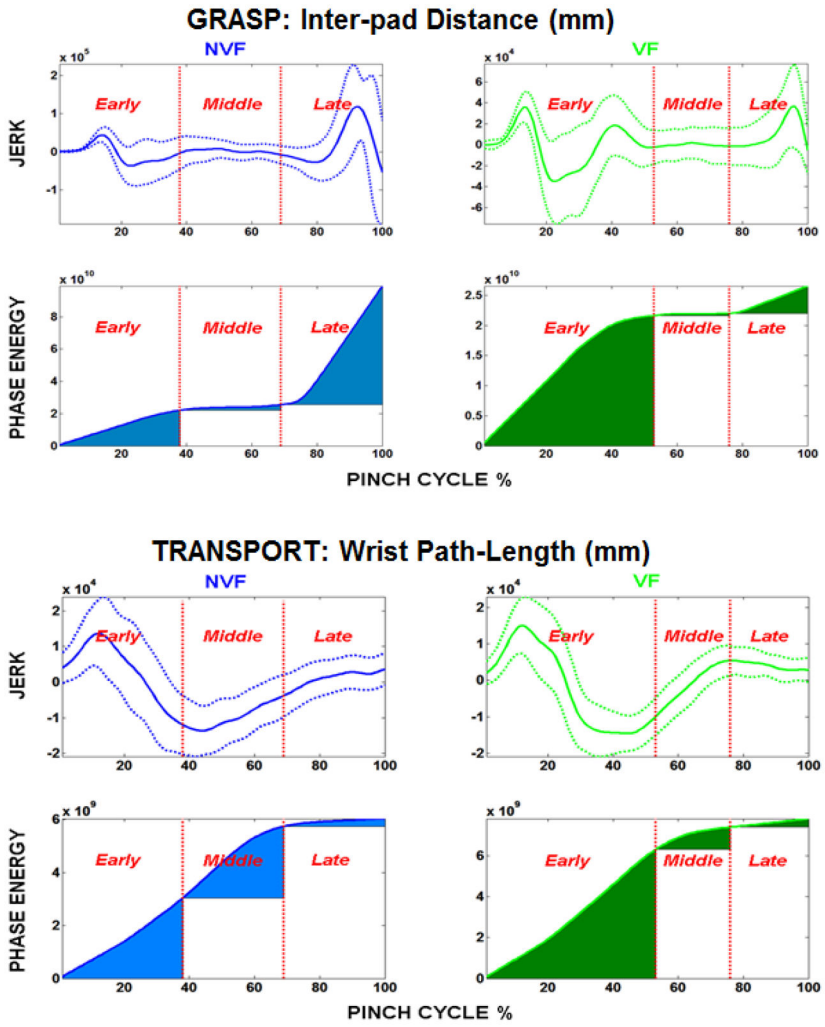

Figure 5.

Jerk trajectory and jerk-energy are shown across observed movement phases (*early*, *middle*, *late*) without (NVF) and with (VF) visual feedback for the grasp variable of inter-pad distance and transport variable of wrist path-length.

Note: (solid line = mean, dotted lines = 1 standard deviation above/below mean)

Note: the units for energy are jerk-squared (i.e., mm^2/sec^6, assuming unitless time-dimension of “pinch cycle”).

Note: The shaded area fills correspond to the cumulative energy binned during the respective movement phase.

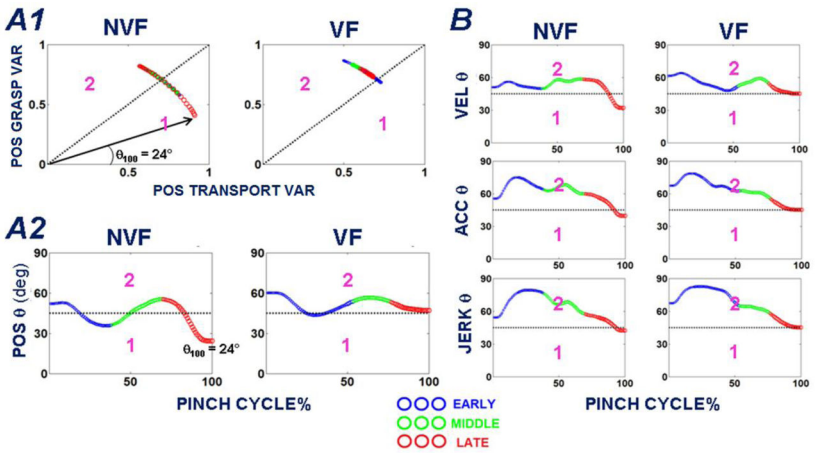

Figure 6.

A1. Relative variability angle (θ) data between grasp and transport used for Markov analysis are shown for position kinematics of representative subject for both visual conditions (NVF, VF). **A2**. Unwrapping relative variability angle across pinch cycle phase (early, middle, late). Each data point assigned to one of two states according to which variability component is greater: State “1” = Transport>Grasp, State “2” = Grasp>Transport **B**. Unwrapped relative variability angle data are shown for velocity, acceleration, and jerk kinematics.

Table 1

Performance Metrics for Grasp (G) and Transport (T) Variables

A1: Trajectory Variability												
	Position			Velocity			Acceleration			Jerk		
VARIABLE	NVF	VF	NVF>VF	NVF	VF	NVF>VF	NVF	VF	NVF>VF	NVF	VF	NVF>VF
Inter-pad Distance, mm (G)	4.9 ±1.6	3.4 ±1.6	+***, (−3.2)	60.2 ±26.5	30.9 ±16.2	+*** (−3.4)	1.47 ±0.75 E+03	7.14 ±3.64 E+02	+*** (−3.4)	4.44 ±2.32 E+04	2.30 ±1.14 E+04	+*** (−3.4)
DOCA – Pitch, deg (G)	8.1 ±6.0	4.5 ±1.8	+** (−2.8)	77.2 ±37.0	41.6 ±16.0	+*** (−3.2)	1.92 ±0.95 E+03	1.04 ±0.39 E+03	+*** (−3.1)	5.81 ±2.81 E+04	3.68 ±1.50 E+04	+* (−2.4)
Wrist Path-Length, mm (T)	12.7 ±3.5	8.3 ±2.6	+** (−3.0)	53.9 ±15.5	36.0 ±11.5	+*** (−3.1)	4.51 ±1.74 E+02	3.50 ±1.33 E+02	+** (−2.8)	7.18 ±3.22 E+03	5.71 ±2.12 E+03	+** (−2.8)

A2: Trajectory Variability Differentials due to Visual Feedback								
	Position		Velocity		Acceleration		Jerk	
VARIABLE	%ΔVF	|ΔG|>|ΔT|	%ΔVF	|ΔG|>|ΔT|	%ΔVF	|ΔG|>|ΔT|	%ΔVF	|ΔG|>|ΔT|
Inter-pad Distance (G)	−31±19	+ (−0.2)	−48±13	+* (−2.2)	−50±13	+*** (−3.2)	−46±14	+*** (−3.4)
DOCA – Pitch (G)	−32±30	+ (−0.1)	−39±26	+ (−1.0)	−37±32	+ (−1.9)	−26±43	+ (−1.0)
Wrist Path-Length (T)	−31±27	n/a	−31±22	n/a	−20±23	n/a	−18±20	n/a

B1: Efficiency: Smoothness			
	Normalized Objective Function Value for Integrated Jerk		
VARIABLE	NVF	VF	NVF>VF
Inter-pad Distance (G)	8.60±5.52 E+05	6.60±5.04 E+05	+* (−2.3)
DOCA – Pitch (G)	3.27±7.02 E+06	7.56±5.02 E+05	+*** (−3.4)
Wrist Path-Length (T)	1.83±3.49 E+05	5.80±12.6 E+04	+* (−1.9)

B2: Smoothness Differentials due to Visual Feedback		
VARIABLE	%ΔVF	|ΔG|>|ΔT|
Inter-pad Distance (G)	−25±58	− (−1.0)
DOCA – Pitch (G)	−43±15	+ (−0.1)
Wrist Path-Length (T)	−40±70	n/a

C1: Efficiency: Phase Energy			
	Integrated Jerk-Squared Binned within Identified Phase		
VARIABLE	**NVF**	**VF**	**NVF>VF**
"Early" Phase Inter-pad Energy (G)	2.04±2.25 E+10	2.52±6.29 E+10	−* (−2.1)
"Middle" Phase Inter-pad Energy (G)	5.21±4.97 E+08	5.93±9.34 E+08	− (−0.1)
"Late" Phase Inter-pad Energy (G)	1.88±3.01 E+10	1.19±1.94 E+09	+*** (−3.5)
***Ratio: Early-to-Late Phase Inter-pad Energy* (G)**	***3.5±7***	***18.7±14***	−*** (−3.4)
"Early" Phase Wrist Energy (T)	1.51±1.62 E+09	1.63±1.61 E+09	− (−1.1)
"Middle" Phase Wrist Energy (T)	3.49±2.47 E+08	3.85±2.33 E+08	− (−1.0)
"Late" Phase Wrist Energy (T)	2.81±6.31 E+08	1.99±2.80 E+08	+ (−1.5)
***Ratio: Early-to-Late Phase Wrist Energy* (T)**	***33.7±53***	***19.1±17***	+ (−1.0)

C2: Phase Energy Ratio Differentials due to Visual Feedback		
VARIABLE	**%ΔVF**	**|ΔG|>|ΔT|**
***Ratio: Early-to-Late Phase Inter-pad Energy* (G)**	434±470	+*** (−3.4)
***Ratio: Early-to-Late Phase Wrist Energy* (T)**	−43±69	n/a

Notes:

- NVF>VF, +/− denotes performance metric value greater/less with no visual feedback
- '*'p<0.05, '**' p<0.01, '***' p<0.001; in parentheses under p-significance is z-value associated with Wilcoxon signed-rank test performed under 'approximate' method
- ΔVF denotes change in performance metric with visual feedback
- |ΔG|>|ΔT| denotes change in grasp performance metric greater than that for transport with visual feedback

Hum Mov Sci. Author manuscript; available in PMC 2015 August 01.

Table 2

Mean Hidden Markov State Self-Transition Probabilities Across All Subjects

	State1			State2		
	NVF	**VF**	**NVF > VF**	**NVF**	**VF**	**NVF > VF**
POS	0.94±0.03	0.91±0.04	+* (−1.9)	0.96±0.01	0.98±0.01	+** (−3.1)
VEL	0.86±0.09	0.79±0.24	+ (−0.6)	0.97±0.04	0.98±0.02	− (−0.3)
ACC	0.78±0.16	0.80±0.17	− (−0.3)	0.99±0.01	0.98±0.01	− (−1.0)
JERK	0.75±0.16	0.80±0.11	− (−1.1)	0.99±0.02	0.98±0.01	+ (−0.24)
trend	*−0.06±0.04*	*−0.03±0.04*	*−* (−2.2)*	*0.010*±0.003	*0.003*±0.001	*+*** (−3.3)*

Notes:

- NVF>VF, +/− denotes performance metric value greater/less with no visual feedback
- “*’ p<0.05, ‘**’ p<0.01, ‘***’ p<0.001; z-value given in parentheses
- Relative variability “states”: State 1 = Transport>Grasp; State 2 = Grasp>Transport
- All reported linear slope-trends are significantly different from zero (p<0.05)

Table 3

Mean Hidden Markov State-Emission Probabilities Across All Subjects

	NVF						VF					
	State 1			State 2			State 1			State 2		
	Early	Middle	Late	Early	Middle	Late	Early	Middle	Late	Early	Middle	Late
POS	0.41	0.22	0.37	0.38	0.34	0.28	0.54	0.21	0.26	0.40	0.33	0.28
VEL	0.28	0.12	0.59	0.36	0.28	0.36	0.35	0.16	0.49	0.44	0.25	0.31
ACC	0.19	0.13	0.68	0.45	0.25	0.30	0.21	0.17	0.62	0.50	0.22	0.28
JERK	0.21	0.11	0.68	0.45	0.25	0.30	0.17	0.16	0.67	0.50	0.25	0.25
trend	***−0.07***	*−0.03*	***0.10***	*0.03*	*−0.03*	*0.01*	***−0.12***	*−0.01*	***0.14***	*0.04*	*−0.03*	*−0.01*

Note:

- Relative variability “states”: State 1 = Transport>Grasp; State 2 = Grasp>Transport
- All linear slope trends are significantly different from zero ($p<0.05$)
- Linear slope-trends>0.05 in magnitude are bolded